IEEE Access
Multidisciplinary | Rapid Review | Open Access Journal

Received May 28, 2020, accepted July 8, 2020, date of publication July 14, 2020, date of current version July 24, 2020.

Digital Object Identifier 10.1109/ACCESS.2020.3009264

Pressure, Flow Rate and Operating Speed Characteristics of a Continuous Flow Left Ventricular Assist Device During Varying Speed Support

SELIM BOZKURT
Institute of Cardiovascular Science, University College London, London WC1E 6BT, U.K.
e-mail: s.bozkurt@ucl.ac.uk

ABSTRACT Hydraulic performance of Continuous Flow Left Ventricular Assist Devices depends on their pressure head and flow rate relations. Hydraulic characteristics of these devices are expressed by pressure head and flow rate loops in a pulsatile environment as they are implanted between left ventricular apex and aorta. Nonetheless, constant speed Continuous Flow Left Ventricular Assist Device support causes complications due to altered blood flow in the patients' body. Therefore, beat-to-beat varying speed Continuous Flow Left Ventricular Assist Device support algorithms have been proposed to operate these devices in synchronized co-pulsating or counter-pulsating modes which can generate more physiological blood flow in the circulatory system. However, the effect of speed variation on the pressure head and flow rate loops remains unclear during varying speed Continuous Flow Left Ventricular Assist Device support. In this study, pressure head, flow rate and operating speed relations during co-pulsating and counter-pulsating pump support in a Continuous Flow Left Ventricular Assist Device were analyzed utilizing numerical simulations. Simulation results show that pressure head - flow rate - operating speed loops can express Continuous Flow Left Ventricular Assist Device characteristics better during varying speed heart pump support. Moreover, pump flow rate - operating speed and pressure head - operating speed diagrams show the dynamic behavior of a heart pump, including also the speed. Therefore, understanding the relationship between speed, flow rate and the pressure difference across a pump may help to develop novel beat-to-beat operating modes to improve Continuous Flow Left Ventricular Assist Device support.

INDEX TERMS Continuous flow left ventricular assist device, hydraulic characteristics, H-Q loops, Q-n loops, H-n loops, H-Q-n loops.

I. INTRODUCTION

Continuous Flow Left Ventricular Assist Devices (CF-LVADs) are used to bridge the time between the decision to transplant and the actual transplantation in end-stage heart failure patients. CF-LVAD hydraulic performance for steady flow depends on the pump pressure head and flow rate (H-Q) characteristics at a certain speed [1]. CF-LVAD H-Q characteristics can be used to estimate the pump flow rate and left ventricular pressure under constant speed pump support [2]. However, CF-LVADs operate in a pulsatile environment because they are implanted between the apex of the left ventricle and ascending aorta, [3]. Pulsatile flow rate and the pressure difference across a CF-LVAD over each cardiac cycle result in CF-LVAD H-Q loops [4].

CF-LVADs support the failing heart by unloading the left ventricle and delivering the blood to aorta continuously by operating at a constant speed [5]. Constant speed CF-LVAD support may cause complications such as remodeling in the blood vessel walls and increased inflammatory response [6], gastrointestinal bleeding in the circulatory system because of reduced arterial pulsatility [7] or aortic valve insufficiency because of altered blood flow in the cardiovascular system [8]. Moreover, optimal left ventricular unloading may not be achieved by constant speed CF-LVAD support because it depends mainly on the cardiac contractions [9]. Therefore, different beat-to-beat co-pulsating and counter-pulsating CF-LVAD support modes to improve arterial

The associate editor coordinating the review of this manuscript and approving it for publication was Chaitanya U. Kshirsagar.

pulsatility [10], [11], coronary perfusion [12], aortic valve function and opening duration [13], left ventricular unloading [14] and myocardial oxygen consumption [15] have been developed [16]. The H-Q characteristics during varying speed CF-LVAD support is affected by the varying pump operating speed along with the pulsating heart [17]. The shape of the H-Q loops during synchronous CF-LVAD support depends on the phase shift and left ventricular contractility still affects the size of CF-LVAD H-Q loop area [17]. Although, CF-LVAD H-Q loops show the head and flow rate relationship in a heart pump and cardiac events occurring during a heartbeat, effects of pump speed variation remain unclear on the H-Q diagram for varying speed CF-LVAD support.

In this study, it is aimed to analyze pressure head (H), flow rate (Q) and operating speed (n) relations in a CF-LVAD using H-n, Q-n and H-Q-n diagrams for varying speed pump support via numerical simulations.

II. MATERIALS AND METHODS

The simulations were performed using a numerical model which describes blood flow rate and pressure in HeartWare HVAD and a cardiovascular system. The cardiovascular system model simulates cardiac function and blood flow in the circulatory system.

HeartWare HVAD is an implantable continuous flow centrifugal pump with magnetic levitation driving system [18], [19]. The recommended operating speed range in the patients for this device is between 2400 rpm and 3200 rpm [20] with 2800 rpm baseline speed [21]. HeartWare HVAD support was simulated using a model which describes CF-LVAD flow rate and the pressure difference across the pump [22] as given below.

$$\begin{aligned} H_{CF-LVAD} &= kn^2_{CF-LVAD} - R_1 n_{CF-LVAD} Q_{CF-LVAD} - R_2 Q^2_{CF-LVAD} \\ &\quad - L_{CF-LVAD} dQ_{CF-LVAD}/dt + H_{rec} \end{aligned} \tag{1}$$

Here, $H_{CF-LVAD}$ and $Q_{CF-LVAD}$ represent pressure head and flow rate, R_1 and R_2 are resistances related with friction and incidence losses, $n_{CF-LVAD}$ is the CF-LVAD operating speed, k is the blood flow source term, $L_{CF-LVAD}$ and H_{rec} are the inertance and part-load recirculation in the pump. Parameter values and the detailed description of the CF-LVAD model can be found in [22].

The cardiovascular system model simulates functions of heart chambers and blood flow in the circulatory system. The ventricle models simulate active and passive contraction phases in the ventricles over a cardiac cycle. The left ventricular pressure (p_{lv}) is described in the cardiovascular system model as given below.

$$p_{lv} = p_{lv,a} + p_{lv,p} \tag{2}$$

$$p_{lv,a}(t) = E_{es,lv}\left(V_{lv} - V_{lv,0}\right) f_{act,lv}(t) \tag{3}$$

$$p_{lv,p} = A\ \exp(B\ V_{lv}) - 1 \tag{4}$$

Here, $p_{lv,a}$ and $p_{lv,p}$ are the active and passive components of the left ventricular pressure, $E_{es,lv}$, and $f_{act,lv}$ are the systolic elastance and activation function in the left ventricle, A and B are coefficients used in the passive left ventricular pressure, V_{lv} and $V_{lv,0}$ are the left ventricular volume and zero-pressure volume. Left ventricular volume (V_{lv}) is simulated as given below.

$$V_{lv} = (2/3)\pi K_{lv} r_{lv}^2 l_{lv} \tag{5}$$

$$\begin{aligned} dr_{lv}/dt &= (3(Q_{mv} - Q_{av}) / (4\pi K_{lv} l_{lv})) \\ &\quad \times (3V_{lv} / (2\pi K_{lv} l_{lv}))^{-1/2} \end{aligned} \tag{6}$$

In the equations above, r_{lv} and l_{lv} are the left ventricular radius and long axis length and K_{lv} is a scaling coefficient. Functions of the right ventricle and atria were simulated using similar models using different parameter values. The circulatory system was modeled using electric analogue models with resistance (R), inertance (L) and compliance (C) properties of the blood vessels. The heart valves were simulated as ideal diodes allowing one-way blood flow. The models used to simulate the change of aortic pressure (p_{ao}) and flow rate (Q_{ao}) with respect to time and flow rate through the aortic valve (Q_{av}) are given below.

$$dp_{ao}/dt = (Q_{av} - Q_{ao})/C_{ao} \tag{7}$$

$$dQ_{ao}/dt = \left(p_{ao} - p_{as} - R_{ao} Q_{ao}\right)/L_{ao} \tag{8}$$

$$Q_{av} = \left(p_{lv} - p_{ao}\right)/R_{av} \tag{9}$$

Here, C_{ao}, R_{ao} and L_{ao} are the compliance, resistance and inertance of the aorta, R_{av} is the aortic valve resistance and p_{as} is the blood pressure in the systemic arterioles. The other compartments in the circulatory system were modeled in the same way using different parameter values. Detailed information about the simulation of cardiac function and circulatory system can be found in [23]. CF-LVAD support was simulated by modifying (6) and (7) as given below.

$$\begin{aligned} dr_{lv}/dt &= \left(3(Q_{mv} - Q_{av} - Q_{CF-LVAD})/(4\pi K_{lv} l_{lv})\right) \\ &\quad \times (3V_{lv}/(2\pi K_{lv} l_{lv}))^{-1/2} \end{aligned} \tag{10}$$

$$dp_{ao}/dt = \left(Q_{av} + Q_{CF-LVAD} - Q_{ao}\right)/C_{ao} \tag{11}$$

Initially, heart failure without CF-LVAD support was simulated using 1.35 mmHg/mL and 0.9 mmHg/mL left ventricular systolic elastance ($E_{es,lv}$) in the cardiovascular system model. The selected $E_{es,lv}$ values allow to simulate partial and full CF-LVAD support. The aortic valve opens over a cardiac cycle at 1.35 mmHg/mL left ventricular systolic elastance, whereas it remains closed at 0.9 mmHg/mL left ventricular systolic elastance during 2800 rpm baseline constant speed CF-LVAD support. Also, left ventricular zero pressure volume ($V_{lv,0}$) was increased to 20 mL from 15 mL, the coefficient A was reduced to 0.85 from 1 and the systemic arteriolar resistance was increased to 1.25 mmHgs/mL from 0.95 mmHgs/mL.

First, CF-LVAD assistance was simulated for 2700 rpm, 2800 rpm and 2900 rpm constant speed pump support. Varying speed CF-LVAD support was simulated adding a sinusoidal speed variation with 200 rpm amplitude to the simulated constant pump speeds over a cardiac cycle.

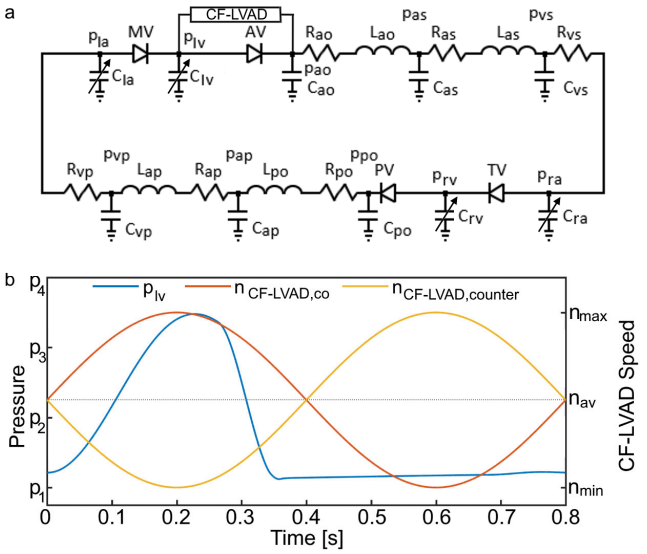

FIGURE 1. a) Electric-analogue of the cardiovascular system model. R, L and C denote resistance, inertance and compliance, p denotes pressure, MV, AV, TV and PV are mitral, aortic, tricuspid and pulmonary valves, la, lv, ra and rv denote left atrium and ventricle and right atrium and ventricle, ao, as, vs denote aorta, systemic arterioles and veins, po, ap, vp pulmonary arteries, pulmonary arterioles and pulmonary veins, b) representative left ventricular pressure (plv) and CF-LVAD operating speed signals for co-pulsating and counter-pulsating pump support (nCF-LVAD,co, nCF-LVAD,counter) over a cardiac cycle. p, nmax, nmin and nav represent pressure, maximal, minimal and average CF-LVAD speeds.

Effect of CF-LVAD operating speed amplitude was evaluated also simulating pump support at 2800 rpm mean speed with 400 rpm amplitude over a cardiac cycle.

Effect of the left ventricular contraction strength on the CF-LVAD H-Q, Q-n, H-n and H-Q-n loops was evaluated using 1.35 mmHg/mL and 0.9 mmHg/mL left ventricular systolic elastances at 2800 rpm mean speed with 200 rpm amplitude over a cardiac cycle.

CF-LVAD speed amplitudes for the varying speed support were selected as 200 rpm and 400 rpm considering the clinically used speed amplitude during Lavare cycle in HeartWare HVAD devices [20].

The speed variation in the CF-LVAD was simulated to provide co-pulsating and counter-pulsating pump support by shifting the speed signal 0.4 s over a cardiac cycle. The varying speed CF-LVAD support over a cardiac cycle was simulated as given below.

$$n_{CF-LVAD} = n_{CF-LVAD,avg} + \sin(2\pi(t - D)/T)\, A_{n,CF-LVAD} \quad (12)$$

Here, $n_{CF-LVAD}$ is the CF-LVAD speed, t is the instantaneous time, D is the delay to shift the pump speed signal, T is the duration of a cardiac cycle and $A_{n,CF-LVAD}$ is the amplitude of the CF-LVAD speed signal. Electric-analogue of the cardiovascular system model, representative left ventricular pressure and CF-LVAD operating speed signals for co-pulsating and counter-pulsating pump support over a cardiac cycle are given in Figure 1.

Duration of a heartbeat was 0.8 s in the simulations. Simulations were performed using Matlab Simulink R2017a. The set of equations was solved using the ode15s solver. The maximum step size was 1e-3 s and the relative tolerance was set to 1e-3.

III. RESULTS

Left ventricular and aortic pressure signals over a cardiac cycle for heart failure and constant speed CF-LVAD support at 2800 rpm for 1.35 mmHg/mL and 0.9 mmHg/mL left ventricular systolic elastance are given in Figure 2.

Cardiac outputs for the heart failure simulated using 1.35 mmHg/mL and 0.9 mmHg/mL left ventricular systolic elastances were 4.39 L/min and 3.67 L/min. Mean flow rate (mean pump output and average flow rate through the aortic valve) in circulatory system at 2800 rpm speed CF-LVAD support for 1.35 mmHg/mL elastance was 5.04 L/min whereas the mean pump output at 2800 rpm speed CF-LVAD support for 0.9 mmHg/mL left ventricular systolic elastances was 4.89 L/min. Cardiac phases in CF-LVAD H-Q loops under constant speed pump support at 2800 rpm and co-pulsating and counter-pulsating pump support at 2800 rpm average speed with 200 rpm speed amplitude over a cardiac cycle and heart failure with 1.35 mmHg/mL left ventricular systolic elastance are given Figure 3.

Point 1 shows the closure of mitral valve and onset of the systolic phase, which are noticeable in the CF-LVAD H-Q loops for all the support modes. Point 2 in the CF-LVAD H-Q loop shows the opening of aortic valve. The pressure difference across CF-LVAD remains constant until the aortic valve closes. Point 3 shows the closure of aortic valve and the beginning of isovolumic relaxation in the left ventricle. Point 4 shows the opening of mitral valve. Cardiac phases in CF-LVAD Q-n, H-n and H-Q-n loops under co-pulsating and counter-pulsating pump support at 2800 rpm average speed with 200 rpm speed amplitude over a cardiac cycle and heart failure with 1.35 mmHg/mL left ventricular systolic elastance are given in Figure 4.

CF-LVAD flow rate decreases sharply after the closure of aortic valve, which is shown with point 3 on the CF-LVAD Q-n loops. The pressure difference across the pump decreases rapidly with the onset of the systole, which is shown with point 1 on the CF-LVAD H-n loops. Ejection phase between point 2 and point 3 is barely noticeable and followed by a rapid increase in the pressure difference across the CF-LVAD. Rapid increase of the differential pump pressure is followed by a plateau which can be seen after the opening of mitral valve on the CF-LVAD H-n loop. Q-n and H-n loops under co-pulsating and counter-pulsating CF-LVAD support have similar shapes, however, flipped horizontally due to phase shift in the pump operating speed over a cardiac cycle. CF-LVAD H-Q loops in the cardiovascular system model simulating heart failure with 1.35 mmHg/mL left ventricular elastance under constant pump speed, co-pulsating and counter-pulsating CF-LVAD support at 2700 rpm, 2800 rpm and 2900 rpm average pump operating speeds over a cardiac cycle are given in Figure 5.

Increasing the average pump operating speed over a cardiac cycle did not change the shape of the CF-LVAD

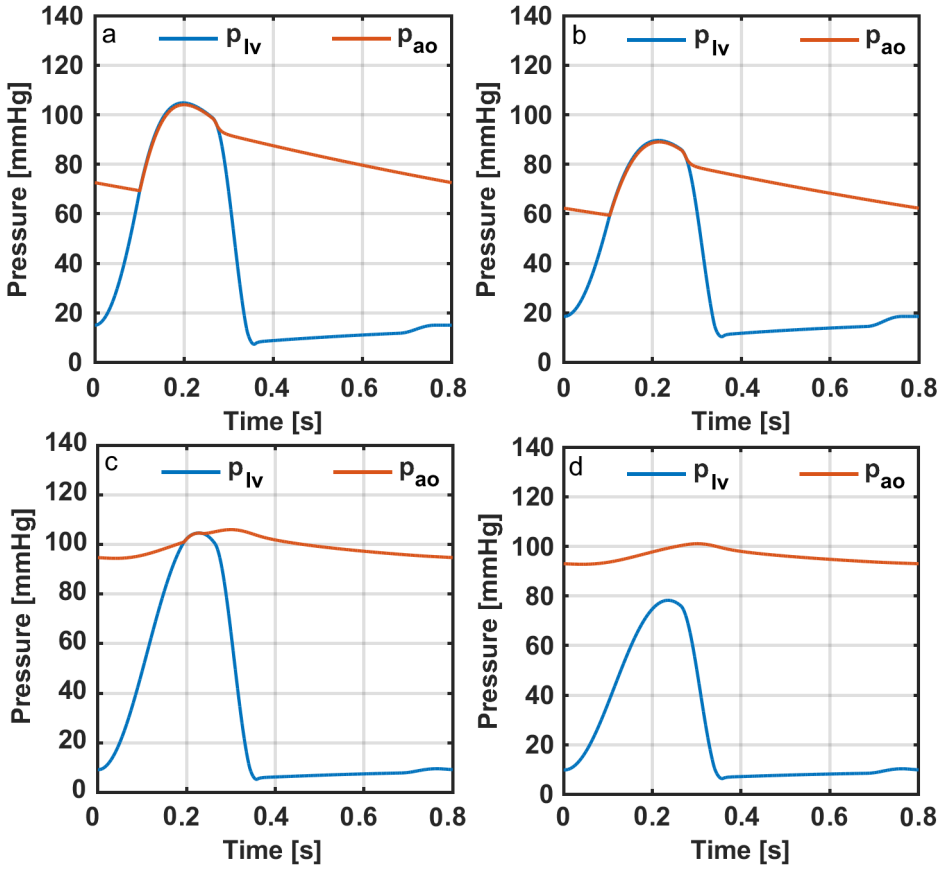

FIGURE 2. a) Left ventricular and aortic pressure signals (plv, pao) over a cardiac cycle for the heart failure simulated using 1.35 mmHg/mL left ventricular elastance, b) plv and pao over a cardiac cycle for the heart failure simulated using 0.9 mmHg/mL left ventricular elastance, c) plv and pao over a cardiac cycle at 2800 rpm constant speed CF-LVAD support for the heart failure simulated using 1.35 mmHg/mL left ventricular elastance, d) plv and pao over a cardiac cycle at 2800 rpm constant speed CF-LVAD support for the heart failure simulated using 0.9 mmHg/mL left ventricular elastance.

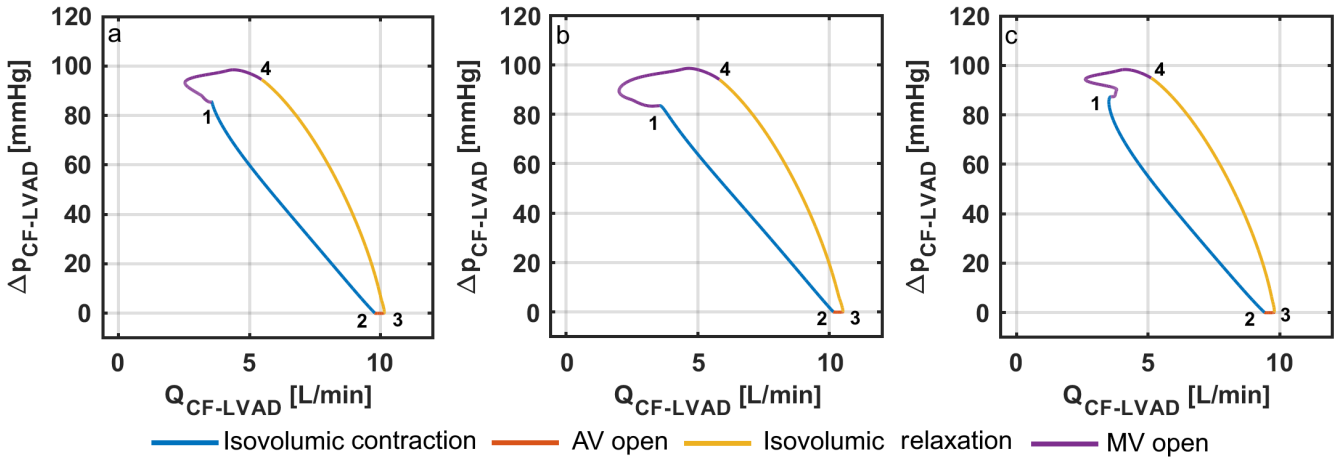

FIGURE 3. Cardiac phases in CF-LVAD H-Q loops for a) 2800 rpm constant speed CF-LVAD support, b) co-pulsating CF-LVAD support at 2800 rpm average speed with 200 rpm amplitude, c) counter-pulsating CF-LVAD support at 2800 rpm average speed with 200 speed rpm amplitude over a cardiac cycle (AV and MV denote aortic and mitral valves).

H-Q loops remarkably, whereas pump H-Q loops shifted to the right. Aortic valve remained closed over a cardiac cycle under CF-LVAD support at 2900 rpm average speed for all the pump operating modes. Therefore, the left ventricular ejection phase disappeared in the CF-LVAD H-Q loops for all the pump support modes. Aortic valve remaining closed over a cardiac cycle did not significantly alter the shape of CF-LVAD. However, it increased the minimal pressure

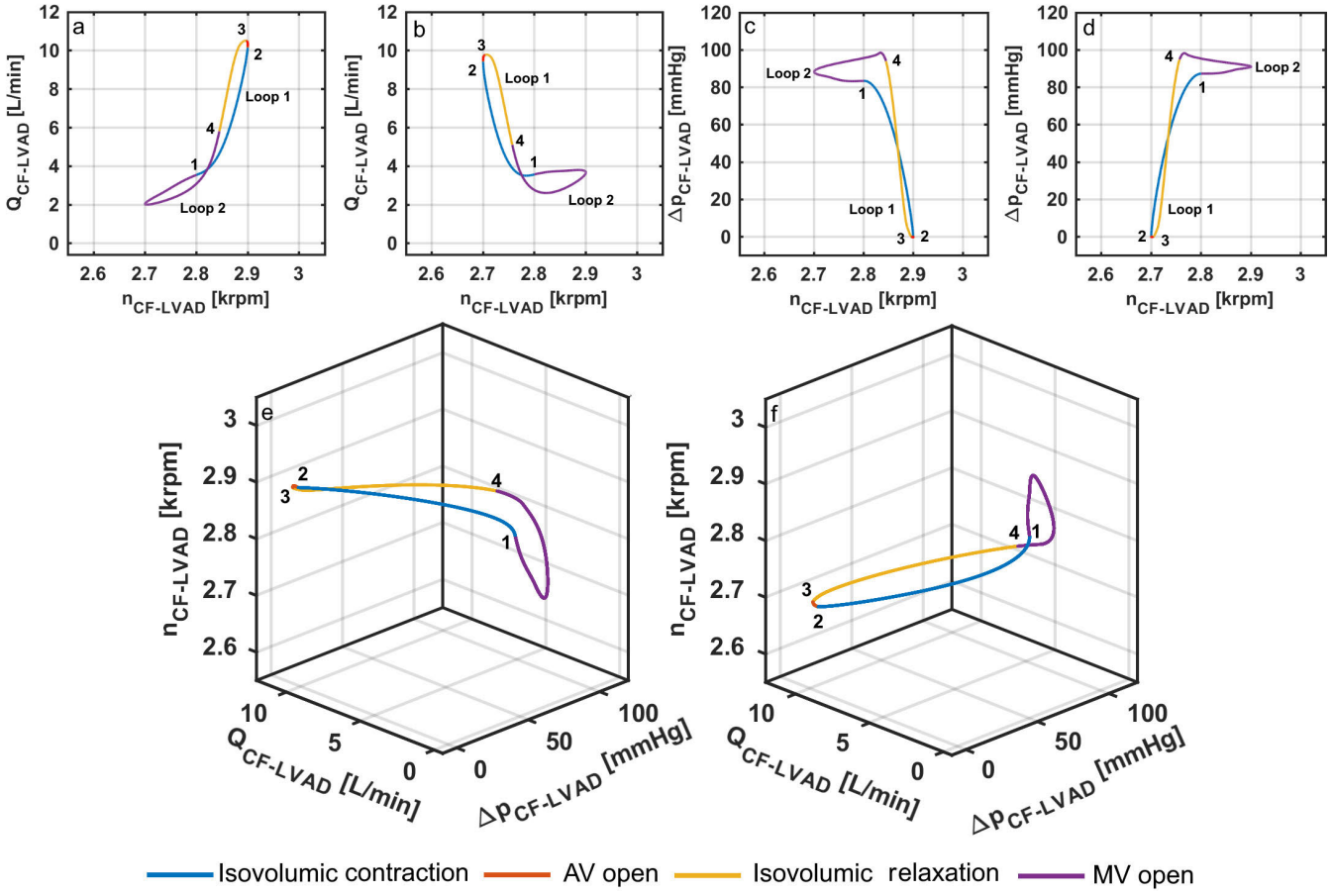

FIGURE 4. Cardiac phases in CF-LVAD Q-n loops for a) co-pulsating CF-LVAD support at 2800 rpm average speed with 200 rpm speed amplitude, b) counter-pulsating CF-LVAD support at 2800 rpm average speed with 200 rpm speed amplitude, cardiac phases in CF-LVAD H-n loops for c) co-pulsating CF-LVAD support at 2800 rpm average speed with 200 speed rpm speed amplitude, d) counter-pulsating CF-LVAD support at 2800 rpm average speed with 200 speed rpm amplitude, cardiac phases in CF-LVAD H-Q-n loops for e) co-pulsating CF-LVAD support at 2800 rpm average speed with 200 rpm speed amplitude, f) counter-pulsating CF-LVAD support at 2800 rpm average speed with 200 rpm speed amplitude over a cardiac cycle (AV and MV represent aortic and mitral valves).

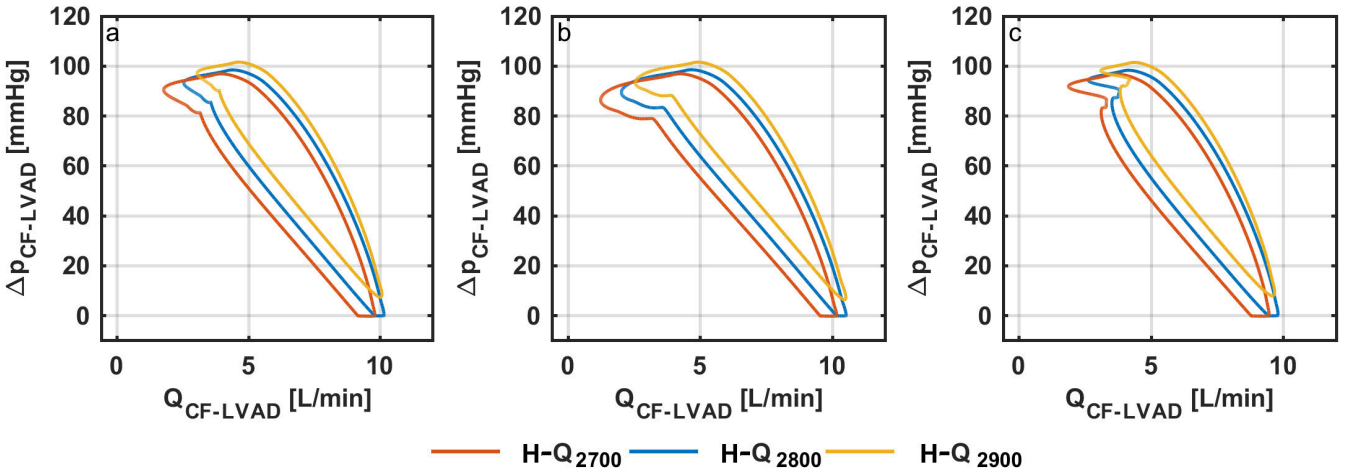

FIGURE 5. CF-LVAD H-Q loops in the cardiovascular system model simulating heart failure with 1.35 mmHg/mL left ventricular elastance under a) constant speed, b) co-pulsating and c) counter-pulsating CF-LVAD support at 2700 rpm (H-Q2700), 2800 rpm (H-Q2800) and 2900 rpm (H-Q2900) average pump operating speeds over a cardiac cycle.

difference across the pump. CF-LVAD Q-n, H-n and H-Q-n loops under co-pulsating and counter-pulsating pump support at 2700 rpm 2800 rpm and 2900 rpm average pump operating speeds with 200 rpm amplitude over a cardiac cycle and heart failure with 1.35 mmHg/mL left ventricular systolic elastance are given in Figure 6.

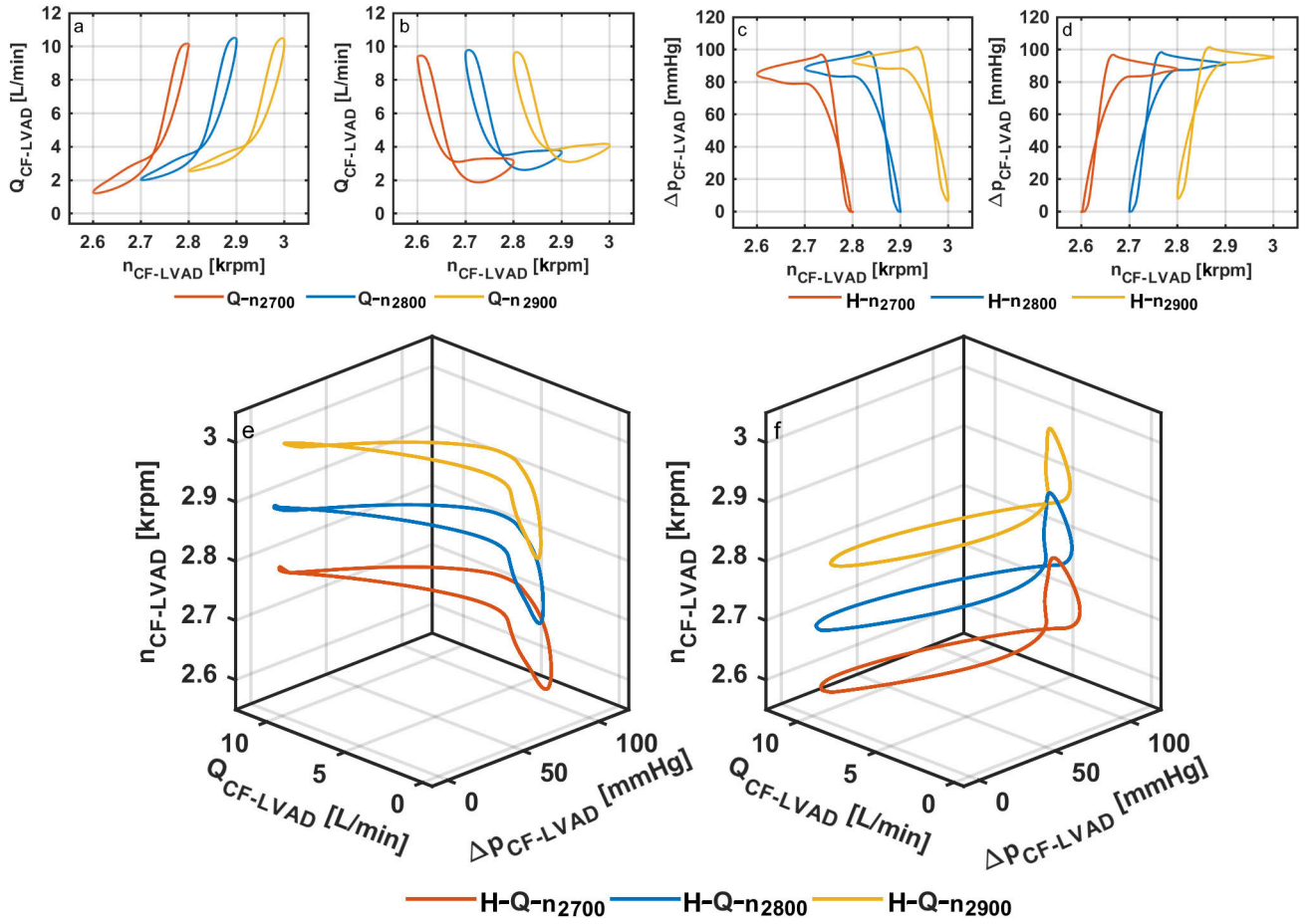

FIGURE 6. CF-LVAD Q-n loops for a) co-pulsating and b) counter-pulsating CF-LVAD support at 2700 rpm (Q-n2700), 2800 rpm (Q-n280) and 2900 rpm (Q-n2900) average pump operating speeds with 200 rpm speed amplitude, CF-LVAD H-n loops for c) co-pulsating and d) counter-pulsating CF-LVAD support at 2700 rpm (H-n2700), 2800 rpm (H-n2800) and 2900 rpm (H-n2900) average pump operating speeds with 200 rpm speed amplitude, CF-LVAD H-Q-n loops for e) co-pulsating and f) counter-pulsating CF-LVAD support at 2700 rpm (H-Q-n2700), 2800 rpm (H-Q-n2800) and 2900 rpm (H-Q-n2900) average pump operating speeds with 200 rpm speed amplitude.

CF-LVAD Q-n and H-n loops shifted right for increasing average pump operating speeds over a cardiac cycle. The pressure difference across pump was around zero in the CF-LVAD H-n loops for the average pump speeds allowing to open the aortic valve over a cardiac cycle. Aortic valve remained closed over a cardiac cycle with the increase of average pump speed to 2900 rpm for both co-pulsating and counter-pulsating support modes. Therefore, the pressure difference across the pump was also increased at the peak systole and the ejection phase did not appear on the CF-LVAD H-n loops at 2900 rpm average pump operating speed (Fig. 6 c,d). Also, CF-LVAD H-Q-n loops under both co-pulsating and counter-pulsating support modes shifted up with the increase in the average pump operating speed over a cardiac cycle. CF-LVAD H-Q loops under constant speed pump support and co-pulsating and counter-pulsating pump support modes for 2800 rpm average operating speed with 200 rpm and 400 rpm speed amplitudes and heart failure with 1.35 mmHg/mL left ventricular systolic elastance are given in Figure 7.

Ejection phase on the CF-LVAD H-Q loop shifted right whereas filling phase extended towards left with the increasing CF-LVAD speed amplitudes under co-pulsating pump support. Increasing the CF-LVAD speed amplitudes over a cardiac cycle shifted ejection phase on the CF-LVAD H-Q loop to the left whereas filling phase looks like a cleft on the CF-LVAD H-Q loop under counter-pulsating pump support. CF-LVAD Q-n, H-n and H-Q-n loops under co-pulsating and counter-pulsating pump support at 2800 rpm average pump operating speed with 200 rpm and 400 rpm amplitudes over a cardiac cycle and heart failure with 1.35 mmHg/mL left ventricular systolic elastance are given in Figure 8.

Increasing the pump speed amplitude during the systolic phase increases the CF-LVAD flow rate during the peak systole under co-pulsating CF-LVAD support. On the other hand, reduced pump operating speed due to a higher pump speed amplitude over the diastolic phase decreased the minimal CF-LVAD flow rate under co-pulsating pump support mode (Fig. 8a). Counter-pulsating pump support did not affect the minimal and maximal CF-LVAD flow rates, whereas the size of the CF-LVAD Q-n loop was relatively large for a higher CF-LVAD speed amplitude over a cardiac cycle (Fig. 8b). Maximal and minimal pressure levels were similar for both

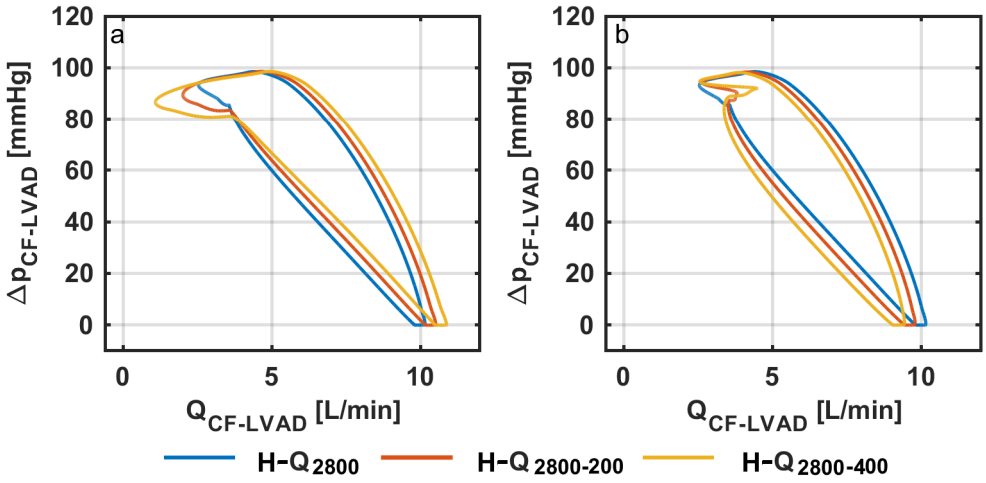

FIGURE 7. CF-LVAD H-Q loops under 2800 rpm constant speed pump support (H-Q2800) and a) co-pulsating and b) counter-pulsating pump support modes for 2800 rpm average operating speed with 200 rpm (H-Q2800-200) and 400 rpm (H-Q2800-400) amplitudes.

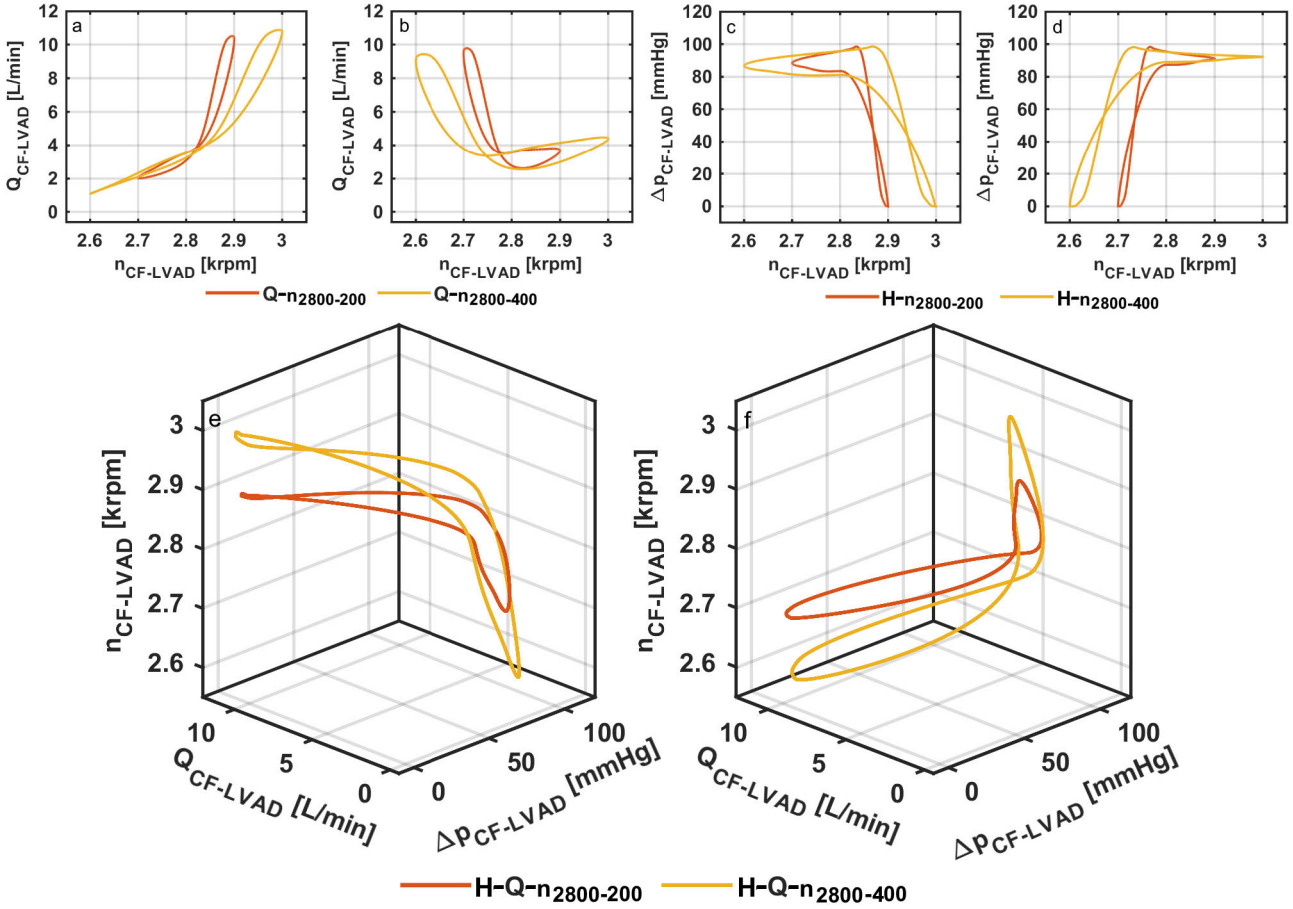

FIGURE 8. CF-LVAD Q-n loops under a) co-pulsating and b) counter-pulsating pump support modes for 2800 rpm average operating speed with 200 rpm (Q-n2800-200) and 400 rpm (Q-n2800-400) amplitudes, CF-LVAD H-n loops under c) co-pulsating and d) counter-pulsating pump support modes for 2800 rpm average operating speed with 200 rpm (H-n2800-200) and 400 rpm (H-n2800-400) amplitudes, CF-LVAD H-Q-n loops under e) co-pulsating and f) counter-pulsating pump support modes for 2800 rpm average operating speed with 200 rpm (H-Q-n2800-200) and 400 rpm (H-Q-n2800-400) amplitudes.

200 rpm and 400 rpm pump speed amplitudes whereas the size of the CF-LVAD H-n loops were larger for 400 rpm pump speed amplitude under co-pulsating and counter-pulsating CF-LVAD support. Here, it should be noted that the average CF-LVAD speed over a cardiac cycle was 2800 rpm allowing the aortic valve to open which plays a role on the minimal pressure and maximal flow rate levels in the CF-LVAD. Co-pulsating pump support shifted the CF-LVAD H-Q-n loop

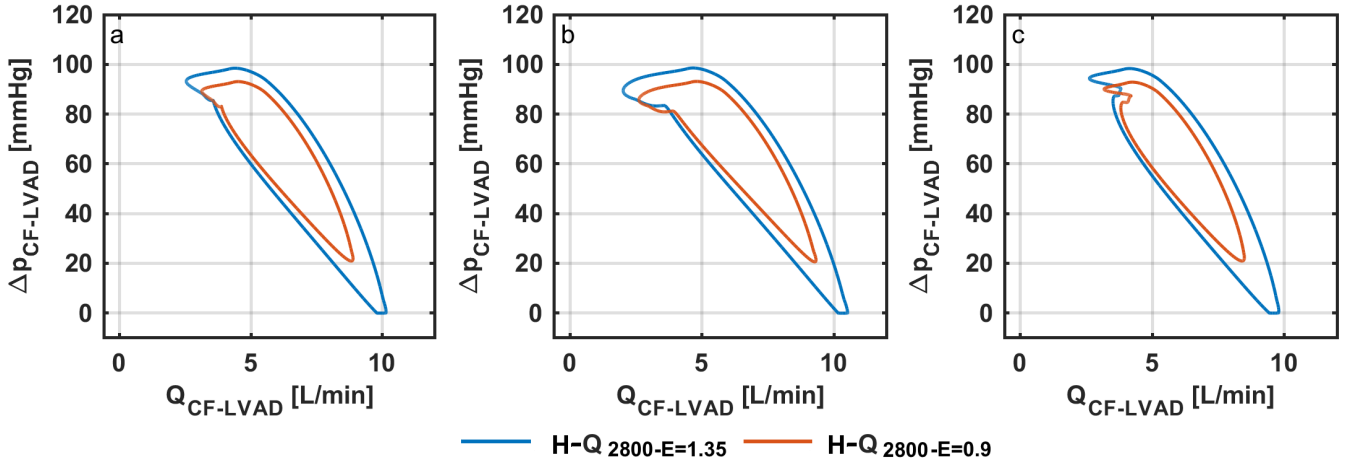

FIGURE 9. CF-LVAD H-Q loops under a) constant speed, b) co-pulsating and c) counter-pulsating pump support modes at 2800 rpm average pump speed over a cardiac cycle with 200 rpm speed amplitude and heart failure with 1.35 mmHg/mL (H-Q2800-E = 1.35) and 0.9 mmHg/mL (H-Q2800-E = 0.9) left ventricular systolic elastances.

up over the systolic phase, whereas the pump flow rate reduced over the diastolic phase (Fig. 8e). Counter-pulsating pump support shifted the CF-LVAD H-Q-n loop down over the systolic phase (Fig. 8f). CF-LVAD H-Q loops under constant speed, co-pulsating and counter-pulsating pump support modes at 2800 rpm average pump speed with 200 rpm speed amplitude and heart failure with 1.35 mmHg/mL and 0.9 mmHg/mL left ventricular systolic elastances are given in Figure 9.

Reducing the left ventricular systolic elastance also decreased the size of CF-LVAD H-Q loop area for all the simulated pump support modes. Moreover, the aortic valve remained closed over a cardiac cycle and aortic valve ejection phase disappeared in the CF-LVAD H-Q loops for heart failure simulated with 0.9 mmHg/mL left ventricular systolic elastance. CF-LVAD Q-n, H-n and H-Q-n loops under co-pulsating and counter-pulsating pump support modes at 2800 rpm average pump speed with 200 rpm speed amplitude and heart failure with 1.35 mmHg/mL and 0.9 mmHg/mL left ventricular systolic elastances are given in Figure 10.

Reduced left ventricular elastance value also reduced the size of the CF-LVAD Q-n, H-Q and H-Q-n loop sizes for both co-pulsating and counter-pulsating pump support modes. CF-LVAD Q-n and H-n loops show that pressure difference across the CF-LVAD increases whereas the pump flow rate decreases for a lower left ventricular elastance at the peak systole for both co-pulsating and counter-pulsating pump support modes because aortic valve remains closed over a cardiac cycle. H-Q, Q-n and H-n loop areas over a cardiac cycle are given in Figure 11.

Increasing the average CF-LVAD speed over a cardiac cycle reduced H-Q loop area for all the pump support modes. Co-pulsating CF-LVAD support generated relatively large H-Q loops. Increasing the speed amplitude in co-pulsating CF-LVAD support mode also increased the H-Q loop area. CF-LVAD H-Q loop area was relatively small for a smaller left ventricular systolic elastance. Increasing average CF-LVAD speed over a cardiac cycle reduced total CF-LVAD Q-n loop area for all the pump support modes. Counter-pulsating CF-LVAD support generated relatively large CF-LVAD Q-n loops. Increasing the speed amplitude in co-pulsating and counter-pulsating CF-LVAD support modes also increased the total Q-n loop area. CF-LVAD Q-n loop area was relatively small for a smaller left ventricular systolic elastance. Increasing average CF-LVAD speed over a cardiac cycle reduced total CF-LVAD H-n loop area for all the pump support modes whereas the area of Loop 1 increased for increasing average CF-LVAD speed over a cardiac cycle. Co-pulsating CF-LVAD support generated relatively large CF-LVAD H-n loops. Increasing the speed amplitude in co-pulsating and counter-pulsating CF-LVAD support modes also increased the total H-n loop area. CF-LVAD H-n loop area was relatively small for a smaller left ventricular systolic elastance. Average CF-LVAD flow rates and the pressure difference across the pump for at 2700 rpm, 2800 rpm and 2900 rpm average CF-LVAD speed with 200 rpm and 400 rpm amplitude under constant speed, co-pulsating and counter-pulsating CF-LVAD support for heart failure with 1.35 mmHg/mL and 0.9 mmHg/mL systolic elastances are given in Table 1.

IV. DISCUSSION

Size and shape of the H-Q loops are affected by the pressure and flow rate characteristics of the pump, contraction strength of the left ventricle and events over a cardiac cycle such as aortic valve opening under constant speed CF-LVAD support [22]. Size and shape of the H-Q loops are also affected by the variation in operating speed of CF-LVADs under varying speed heart pump support [17]. Effect of the speed variation on the shape of the H-Q loop is noticeable over the diastolic phase, which is shown between point 4 and point 1 (Fig. 3). Shape of the CF-LVAD H-Q loops under varying speed support becomes different with respect to the shape of the H-Q loops generated under constant speed

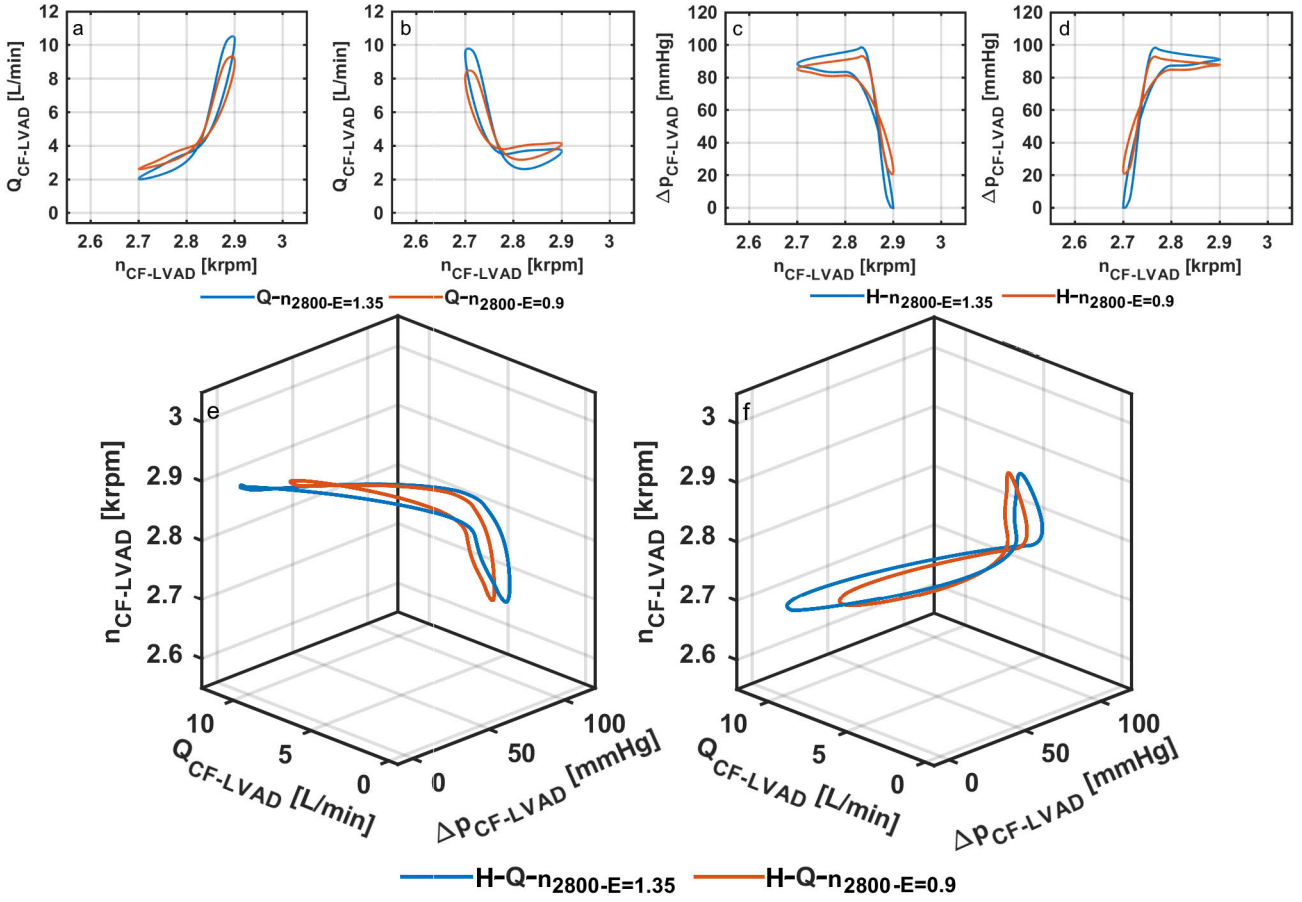

FIGURE 10. CF-LVAD Q-n loops under a) co-pulsating and b) counter-pulsating pump support modes at 2800 rpm average pump speed over a cardiac cycle with 200 rpm speed amplitude and heart failure with 1.35 mmHg/mL (Q-n2800-E = 1.35) and 0.9 mmHg/mL (Q-n2800-E = 0.9) left ventricular systolic elastances, CF-LVAD H-n loops under c) co-pulsating and d) counter-pulsating pump support modes at 2800 rpm average pump speed over a cardiac cycle with 200 rpm speed amplitude and heart failure with 1.35 mmHg/mL (H-n2800-E = 1.35) and 0.9 mmHg/mL (H-n2800-E = 0.9) left ventricular systolic elastances, CF-LVAD H-Q-n loops under e) co-pulsating and f) counter-pulsating pump support modes at 2800 rpm average pump speed over a cardiac cycle with 200 rpm speed amplitude and heart failure with 1.35 mmHg/mL (H-Q-n2800-E = 1.35) and 0.9 mmHg/mL (H-Q-n2800-E = 0.9) left ventricular systolic elastances.

CF-LVAD support. Because CF-LVADs do not operate around a standard H-Q loop during a varying speed heart pump support. Simulation results show that the generated H-Q loops under varying speed CF-LVAD support are the projections of H-Q-n loops on the H-Q plane. Therefore, the effect of the pump speed variation on an H-Q diagram for a varying speed CF-LVAD support algorithm may remain unclear. On the other hand, CF-LVAD Q-n and H-n diagrams show the pump speed variation together with pump flow rate and pressure difference across the pump.

CF-LVAD Q-n and H-n loops are generated during varying speed heart pump support. Size and shape of the CF-LVAD Q-n and H-n loops are affected by the pressure and flow rate characteristics of the pump, contraction strength of left ventricle and the applied speed variation. Opening of the aortic valve did not have any noticeable effects on the shape of CF-LVAD Q-n loops whereas minimal pressure difference across the pump was increased when the aortic valve remained closed over a cardiac cycle due to relatively high average pump speed (Fig. 6) or low left ventricular systolic elastance (Fig. 10). CF-LVAD speed variation over a cardiac cycle also affected the shape and size of the Q-n and H-n loops. Counter-pulsating CF-LVAD support generated relatively large pump Q-n loops for the same average pump speed and speed amplitude over a cardiac cycle. This becomes more apparent for relatively high CF-LVAD speed amplitudes during counter-pulsating pump support (Fig. 11b). Such a result suggests that CF-LVAD speed increase over the diastolic phase can generate a higher variation in pump flow rate over a cardiac cycle. Co-pulsating CF-LVAD support generated relatively large pump H-n loops for the same average pump speed and speed amplitude over a cardiac cycle. This result suggests that increasing the CF-LVAD speed over systolic phase generates a higher variation in pressure difference across the pump over a cardiac cycle.

Left ventricular systolic elastance also plays a role on size of the CF-LVAD H-Q, Q-n and H-n loops. However, it does not affect the shape of these loops significantly. Areas of the CF-LVAD H-Q, Q-n and H-n loops become larger for relatively high left ventricular systolic elastances.

CF-LVAD H-Q-n loops show the variation of CF-LVAD flow rate, pressure difference across the CF-LVAD and

TABLE 1. Average CF-LVAD flow rates and pressure differences across the pump at 2700 RPM, 2800 RPM and 2900 RPM average CF-LVAD speed with 200 RPM and 400 RPM amplitude under constant speed, co-pulsating and counter-pulsating (CS, Co, Cou) CF-LVAD support for heart failure with 1.35 mmHg/mL and 0.9 mmHg/mL systolic elastances.

CF-LVAD Support Mode	CF-LVAD Operating Speed [rpm]	CF-LVAD Speed Amplitude [rpm]	LV Systolic Elastance [mmHg/mL]	CF-LVAD Flow Rate [L/min]	CF-LVAD Pressure [mmHg]
CS	2700	-	1.35	4.49	64.6
CS	2800	-	1.35	4.95	67.9
CS	2900	-	1.35	5.20	73.3
Co	2700	200	1.35	4.40	63.5
Co	2800	200	1.35	4.88	66.9
Co	2900	200	1.35	5.16	72.2
Cou	2700	200	1.35	4.56	65.5
Cou	2800	200	1.35	5.00	68.8
Cou	2900	200	1.35	5.23	74.3
Co	2800	400	1.35	4.78	65.7
Cou	2800	400	1.35	5.04	69.5
CS	2800	-	0.9	4.89	71.0
Co	2800	200	0.9	4.85	70.0
Cou	2800	200	0.9	4.92	71.7

operating speed over a cardiac cycle; therefore, they provide a complete representation of hydraulic CF-LVAD characteristics for varying speed heart pump support. Changes of the pump flow rate and pressure difference under co-pulsating and counter-pulsating support are in the same direction in the CF-LVAD H-Q-n loops (Fig. 4e, 4f). Therefore, contraction and relaxation behaviors of the left ventricle have a significant influence on the pump flow rate and pressure difference signals. Effect of the phase difference in the CF-LVAD operating speed can be seen on the orientations of CF-LVAD H-Q-n loops. CF-LVAD operating speed amplitude affects the size of the pump H-Q-n curves. Moreover, a higher speed amplitude shifts CF-LVAD H-Q-n loops on the speed axis up or down depending on the pump support mode.

Dynamic pump H-Q characteristics under constant speed CF-LVAD support have been investigated to estimate the pump flow rate by Pennings *et al.* [24]. It has been found that static H-Q characteristics provide only a basis for the estimation for the CF-LVAD flow. Therefore, dynamic pump H-Q characteristics which are generated because of beating left ventricle needs to be used to estimate the flow rate more accurately [24]. The simulation results show that the H-Q loop area depends on the variation of pump speed under varying speed CF-LVAD support. Therefore, CF-LVAD Q-n and H-n characteristics need to be considered as well for the proposed varying speed CF-LVAD support modes to estimate the pump variables. Another study by Graefe *et al.* [25] found that CF-LVAD H-Q characteristics play a role on the unloading of the left ventricle during exercise, therefore, sustaining exercise capacity of a failing heart also depends on the CF-LVAD H-Q characteristics under constant speed

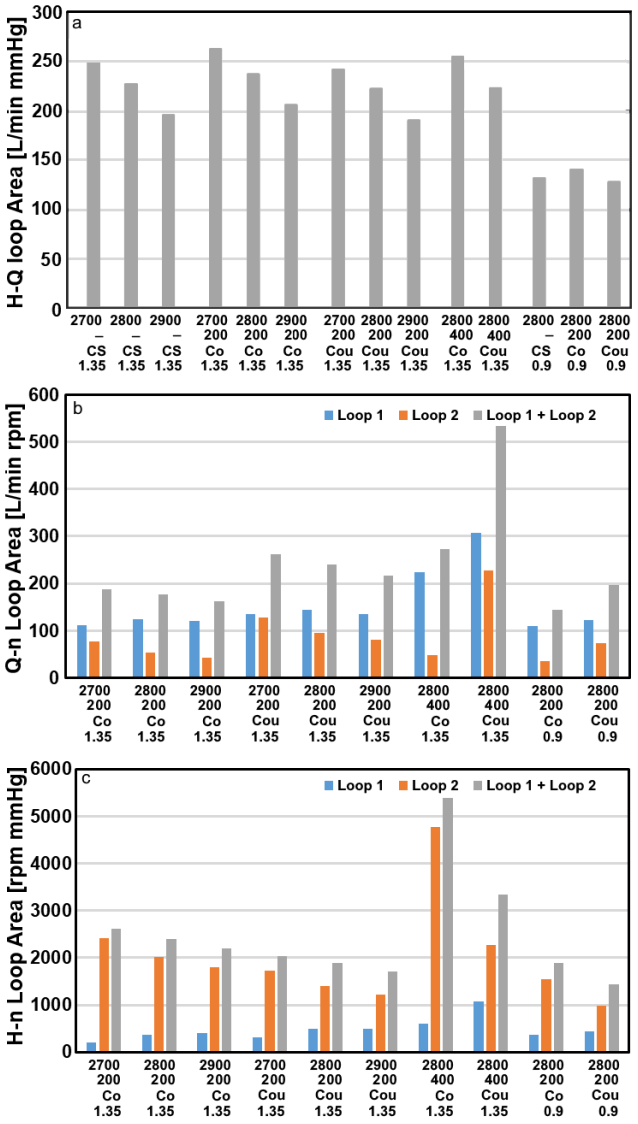

FIGURE 11. a) CF-LVAD H-Q loop area at 2700 rpm, 2800 rpm and 2900 rpm (2700, 2800, 2900) average speed with 200 rpm and 400 rpm speed amplitude (200, 400) under constant speed, co-pulsating and counter-pulsating (CS, Co, Cou) CF-LVAD support for heart failure with 1.35 mmHg/mL and 0.9 mmHg/mL (1.35, 0.9) systolic elastances, b) CF-LVAD Q-n loop area at 2700 rpm, 2800 rpm and 2900 rpm (2700, 2800, 2900) average speed with 200 rpm and 400 rpm speed amplitude (200, 400) under co-pulsating and counter-pulsating (Co, Cou) CF-LVAD support for heart failure with 1.35 mmHg/mL and 0.9 mmHg/mL (1.35, 0.9) systolic elastances, c) CF-LVAD H-n loop area at 2700 rpm, 2800 rpm and 2900 rpm (2700, 2800, 2900) average speed with 200 rpm and 400 rpm speed amplitude (200, 400) under co-pulsating and counter-pulsating (Co, Cou) CF-LVAD support for heart failure with 1.35 mmHg/mL and 0.9 mmHg/mL (1.35, 0.9) systolic elastances.

pump support. CF-LVAD pressure sensitivity also plays a role on the left ventricular unloading, thus afterload of the right ventricle [26]. Severe mitral insufficiency may increase the right ventricular afterload as well [26]. It has already been shown that changing the CF-LVAD operating speed continuously over a cardiac cycle may improve the unloading of the left ventricle [27]. Unloading of the left ventricle with mitral valve insufficiency under varying speed CF-LVAD support will also depend on the pump speed variation. So, the effect

of the speed variation on the unloading of the left ventricle during different hemodynamic states needs to be investigated along with the pump H-Q characteristics. CF-LVAD Q-n and H-n loops may help to understand the dynamic behavior of a pump during different hemodynamic states. Here, it should be noted that ideal diodes were used as heart valve models in the simulations. More elaborated models simulating reverse flow through the heart valves will allow to analyze heart valve insufficiency in a more realistic way.

Varying speed CF-LVAD support have implications on the cardiac function and blood flow in the circulatory system. Left ventricular unloading is improved under counter-pulsating CF-LVAD support [27]. Aortic valve opening duration and coronary perfusion are also increased under counter-pulsating CF-LVAD support [12], [28]. Arterial pulsatility is increased under co-pulsating CF-LVAD support [29]. Therefore, physiologic implications of varying speed CF-LVAD support have been known [30]. However, optimal hemodynamic outcome from the varying speed CF-LVAD support for different purposes requires further research. Therefore, CF-LVAD Q-n, H-n and H-Q-n loops investigated in this study may help to develop varying speed CF-LVAD support algorithms which can improve the outcome of heart pump therapy.

Although shape and size of H-Q loops in different CF-LVADs resemble each other, H-Q characteristics of CF-LVADs are different in each device, therefore, H-Q loop shapes and sizes for each CF-LVAD are also slightly different under same conditions [31]. Similar differences can also be expected in Q-n and H-n loop characteristics for different CF-LVADs. Moreover, different CF-LVAD speed variation algorithms will generate different size and shape Q-n and H-n loops. Therefore, analyzing pressure, flow rate and operating speed characteristics of CF-LVADs also requires to analyze H-Q, Q-n and H-n loops for each varying speed CF-LVAD mode separately.

Co-pulsating and counter-pulsating CF-LVAD support require synchronization of heart beats and pump speed signals over each cardiac cycle. R wave in the natural ECG has a very sharp peak at the beginning of the systolic phase. This peak is used for synchronization purposes in clinics, for MR or CT imaging. Synchronizing a pump with this signal may be feasible in real applications.

V. CONCLUSION

CF-LVAD H-Q loops reveal hydraulic characteristics of heart pump only under constant speed CF-LVAD support. However, proposed CF-LVAD speed variation algorithms aiming to alleviate the harmful effects of the constant speed pump support change CF-LVAD speed continuously over a cardiac cycle. CF-LVAD Q-n, H-n and H-Q-n diagrams show the dynamic behavior of a pump including also the speed. Therefore, understanding the relationship between speed, flow rate and the pressure difference across a pump may help to develop novel pump operating modes to improve CF-LVAD support.

REFERENCES

[1] N. Moazami, K. Fukamachi, M. Kobayashi, N. G. Smedira, K. J. Hoercher, A. Massiello, S. Lee, D. J. Horvath, and R. C. Starling, "Axial and centrifugal continuous-flow rotary pumps: A translation from pump mechanics to clinical practice," *J. Heart Lung Transplantation*, vol. 32, no. 1, pp. 1–11, Jan. 2013, doi: 10.1016/j.healun.2012.10.001.

[2] K. A. M. A. Pennings, S. van Tuijl, F. N. van de Vosse, B. A. J. de Mol, and M. C. M. Rutten, "Estimation of left ventricular pressure with the pump as–sensor–in patients with a continuous flow LVAD," *Int. J. Artif. Organs*, vol. 38, no. 8, pp. 433–443, Aug. 2015, doi: 10.5301/ijao.5000424.

[3] M. S. Slaughter, F. D. Pagani, J. G. Rogers, L. W. Miller, B. Sun, S. D. Russell, R. C. Starling, L. Chen, A. J. Boyle, S. Chillcott, R. M. Adamson, M. S. Blood, M. T. Camacho, K. A. Idrissi, M. Petty, M. Sobieski, S. Wright, T. J. Myers, and D. J. Farrar, "Clinical management of continuous-flow left ventricular assist devices in advanced heart failure," *J. Heart Lung Transplantation*, vol. 29, no. 4, pp. 1–39, Apr. 2010, doi: 10.1016/j.healun.2010.01.011.

[4] T. Pirbodaghi, A. Weber, T. Carrel, and S. Vandenberghe, "Effect of pulsatility on the mathematical modeling of rotary blood pumps," *Artif. Organs*, vol. 35, no. 8, pp. 825–832, Aug. 2011, doi: 10.1111/j.1525-1594.2011.01276.x.

[5] D. Mancini and P. C. Colombo, "Left ventricular assist devices," *J. Amer. College Cardiol.*, vol. 65, no. 23, pp. 2542–2555, Jun. 2015, doi: 10.1016/j.jacc.2015.04.039.

[6] B. Ji and A. Andar, "An evaluation of the benefits of pulsatile versus nonpulsatile perfusion during cardiopulmonary bypass procedures in pediatric and adult cardiac patients," *ASAIO J.*, vol. 52, no. 4, pp. 357–361, Jul. 2006, doi: 10.1097/01.mat.0000225266.80021.9b.

[7] F. Vincent, "Arterial pulsatility and circulating von willebrand factor in patients on mechanical circulatory support," *J. Amer. College Cardiol.*, vol. 71, no. 19, pp. 2106–2118, May 2018, doi: 10.1016/j.jacc.2018.02.075.

[8] R. John, K. Mantz, P. Eckman, A. Rose, and K. May-Newman, "Aortic valve pathophysiology during left ventricular assist device support," *J. Heart Lung Transplantation*, vol. 29, no. 12, pp. 1321–1329, Dec. 2010, doi: 10.1016/j.healun.2010.06.006.

[9] S. Vandenberghe, P. Segers, B. Meyns, and P. Verdonck, "Unloading effect of a rotary blood pump assessed by mathematical modeling," *Artif. Organs*, vol. 27, no. 12, pp. 1094–1101, Dec. 2003, doi: 10.1111/j.1525-1594.2003.07198.x.

[10] K. G. Soucy, G. A. Giridharan, Y. Choi, M. A. Sobieski, G. Monreal, A. Cheng, E. Schumer, M. S. Slaughter, and S. C. Koenig, "Rotary pump speed modulation for generating pulsatile flow and phasic left ventricular volume unloading in a bovine model of chronic ischemic heart failure," *J. Heart Lung Transplantation*, vol. 34, no. 1, pp. 122–131, Jan. 2015, doi: 10.1016/j.healun.2014.09.017.

[11] S. Bozkurt, S. van Tuijl, F. N. van de Vosse, and M. C. M. Rutten, "Arterial pulsatility under phasic left ventricular assist device support," *Bio-Med. Mater. Eng.*, vol. 27, no. 5, pp. 451–460, Nov. 2016, doi: 10.3233/BME-161599.

[12] L. G. E. Cox, S. Loerakker, M. C. M. Rutten, B. A. J. M. de Mol, and F. N. van de Vosse, "A mathematical model to evaluate control strategies for mechanical circulatory support," *Artif. Organs*, vol. 33, no. 8, pp. 593–603, Aug. 2009, doi: 10.1111/j.1525-1594.2009.00755.x.

[13] Y. Kishimoto, Y. Takewa, M. Arakawa, A. Umeki, M. Ando, T. Nishimura, Y. Fujii, T. Mizuno, M. Nishimura, and E. Tatsumi, "Development of a novel drive mode to prevent aortic insufficiency during continuous-flow LVAD support by synchronizing rotational speed with heartbeat," *J. Artif. Organs*, vol. 16, no. 2, pp. 129–137, Jun. 2013, doi: 10.1007/s10047-012-0685-x.

[14] D. Ogawa, S. Kobayashi, K. Yamazaki, T. Motomura, T. Nishimura, J. Shimamura, T. Tsukiya, T. Mizuno, Y. Takewa, and E. Tatsumi, "Mathematical evaluation of cardiac beat synchronization control used for a rotary blood pump," *J. Artif. Organs*, vol. 22, no. 4, pp. 276–285, Dec. 2019, doi: 10.1007/s10047-019-01117-3.

[15] A. Umeki, T. Nishimura, Y. Takewa, M. Ando, M. Arakawa, Y. Kishimoto, T. Tsukiya, T. Mizuno, S. Kyo, M. Ono, Y. Taenaka, and E. Tatsumi, "Change in myocardial oxygen consumption employing continuous-flow LVAD with cardiac beat synchronizing system, in acute ischemic heart failure models," *J. Artif. Organs*, vol. 16, no. 2, pp. 119–128, Jun. 2013, doi: 10.1007/s10047-012-0682-0.

[16] S. Bozkurt, "Physiologic outcome of varying speed rotary blood pump support algorithms: A review study," *Australas. Phys. Eng. Sci. Med.*, vol. 39, no. 1, pp. 13–28, Mar. 2016, doi: 10.1007/s13246-015-0405-y.

[17] S. E. Jahren, G. Ochsner, F. Shu, R. Amacher, J. F. Antaki, and S. Vandenberghe, "Analysis of pressure head-flow loops of pulsatile rotodynamic blood pumps," *Artif. Organs*, vol. 38, no. 4, pp. 316–326, Apr. 2014, doi: 10.1111/aor.12139.

[18] J. A. LaRose, D. Tamez, M. Ashenuga, and C. Reyes, "Design concepts and principle of operation of the HeartWare ventricular assist system," *ASAIO J.*, vol. 56, no. 4, pp. 285–289, Jul. 2010, doi: 10.1097/MAT.0b013e3181dfbab5.

[19] C. S. Hayward and M. Swartz. (Jan. 2012). *The Evolution of Ventricular Assist Devices and the Heartware Ventricular Assist System*. Accessed: Apr. 12, 2020. [Online]. Available: https://www.ecrjournal.com/articles/HeartWare-Ventricular-Assist-System

[20] *HeartWare TMHVADTM System*, Heartware, Framingham, MA, USA, 2018.

[21] M. T. Hosseini, A. F. Popov, A. R. Simon, M. Amrani, and T. Bahrami, "Comparison of left ventricular geometry after heart mate II and heartware left ventricular assist device implantation," *J. Cardiothoracic Surg.*, vol. 8, no. 1, p. 31, Feb. 2013, doi: 10.1186/1749-8090-8-31.

[22] S. Boes, B. Thamsen, M. Haas, M. S. Daners, M. Meboldt, and M. Granegger, "Hydraulic characterization of implantable rotary blood pumps," *IEEE Trans. Biomed. Eng.*, vol. 66, no. 6, pp. 1618–1627, Jun. 2019, doi: 10.1109/TBME.2018.2876840.

[23] S. Bozkurt, "Mathematical modeling of cardiac function to evaluate clinical cases in adults and children," *PLoS ONE*, vol. 14, no. 10, Oct. 2019, Art. no. e0224663, doi: 10.1371/journal.pone.0224663.

[24] K. A. M. A. Pennings, J. R. Martina, B. F. M. Rodermans, J. R. Lahpor, F. N. van de Vosse, B. A. J. M. de Mol, and M. C. M. Rutten, "Pump flow estimation from pressure head and power uptake for the heart assist5, heart mate II, and heart ware VADs," *ASAIO J.*, vol. 59, no. 4, pp. 420–426, 2013, doi: 10.1097/MAT.0b013e3182937a3a.

[25] R. Graefe, A. Henseler, R. Körfer, B. Meyns, and L. Fresiello, "Influence of left ventricular assist device pressure-flow characteristic on exercise physiology: Assessment with a verified numerical model," *Int. J. Artif. Organs*, vol. 42, no. 9, pp. 490–499, Sep. 2019, doi: 10.1177/0391398819846126.

[26] R. Graefe, C. Beyel, A. Henseler, R. Körfer, U. Steinseifer, and G. Tenderich, "The effect of LVAD pressure sensitivity on the assisted circulation under consideration of a mitral insufficiency: An *in vitro* study," *Artif. Organs*, vol. 42, no. 10, pp. E304–E314, Oct. 2018, doi: 10.1111/aor.13279.

[27] S. Bozkurt and S. Bozkurt, "In-silico evaluation of left ventricular unloading under varying speed continuous flow left ventricular assist device support," *Biocyber. Biomed. Eng.*, vol. 37, no. 3, pp. 373–387, 2017, doi: 10.1016/j.bbe.2017.03.003.

[28] B. Gao and Q. Zhang, "Biomechanical effects of the working modes of LVADs on the aortic valve: A primary numerical study," *Comput. Methods Programs Biomed.*, vol. 193, Sep. 2020, Art. no. 105512, doi: 10.1016/j.cmpb.2020.105512.

[29] M. Ising, S. Warren, M. A. Sobieski, M. S. Slaughter, S. C. Koenig, and G. A. Giridharan, "Flow modulation algorithms for continuous flow left ventricular assist devices to increase vascular pulsatility: A computer simulation study," *Cardiovasc. Eng. Tech.*, vol. 2, no. 2, p. 90, Mar. 2011, doi: 10.1007/s13239-011-0042-x.

[30] V. Tchantchaleishvili, J. G. Y. Luc, C. M. Cohan, K. Phan, L. Häbbert, S. W. Day, and H. T. Massey, "Clinical implications of physiologic flow adjustment in continuous-flow left ventricular assist devices," *ASAIO J.*, vol. 63, no. 3, pp. 241–250, 2017, doi: 10.1097/MAT.0000000000000477.

[31] M. R. Noor, C. H. Ho, K. H. Parker, A. R. Simon, N. R. Banner, and C. T. Bowles, "Investigation of the characteristics of heartware HVAD and thoratec heartmate II under steady and pulsatile flow conditions," *Artif. Organs*, vol. 40, no. 6, pp. 549–560, Jun. 2016, doi: 10.1111/aor.12593.

SELIM BOZKURT received the Ph.D. degree from the Eindhoven University of Technology, in 2014. He is currently a Research Associate with the Institute of Cardiovascular Sciences, University College London. His research interests include design, testing, and analyzing medical devices for cardiovascular systems and simulation of surgical procedures in patients with cranial anomalies.